

Syntheses, Structural Characterization, and Properties of Ag(I) Complexes from Oxazoline-Based Ligands¹

H. W. Kuai^a, *^a, Y. H. Qian^a, T. Hu^a, and D. Y. Jiang^a

^aFaculty of Chemical Engineering, Huaiyin Institute of Technology, Huai'an, 223003 P.R. China

*e-mail: hyitshy@126.com

Received December 8, 2017

Abstract—The reactions of 2,6-di(2-oxazolyl)pyridine (L^1), 2-[(*S*)-4-phenyl-2-oxazolyl]quinoline (L^2) and 2-[(*S*)-4-isopropyl-2-oxazolyl]quinoline (L^3) with silver nitrate yield three new complexes $\{[Ag_5(L^1)_5](NO_3)_5\}_n$ (**I**), $[Ag(L^2)(NO_3)]$ (**II**), and $[Ag(L^3)(NO_3)(CH_3CN)]$ (**III**), which have been fully characterized by single-crystal X-ray diffraction (CIF files nos. 1553091, 1553092, and 1559788, respectively), IR spectroscopy, and elemental and thermogravimetric analyses. Complex **I** shows a helical chain structure and the spiral directions of the chains are opposite, resulting in an achiral meso structure. Both **II** and **III** display discrete mononuclear structures. Fluorescence and non-linear optical (NLO) properties of the complexes were investigated.

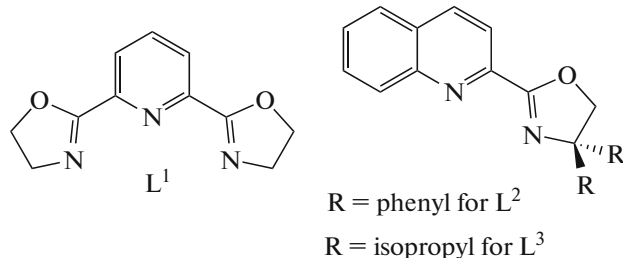
Keywords: silver(I), oxazoline, helical chain, fluorescence, NLO properties

DOI: 10.1134/S107032841809004X

INTRODUCTION

Metal oxazoline complexes possess potential applications in many fields, such as optical materials, which thus attracted increasing interest in coordination and organometallic chemistry [1]. In previous report, oxazoline-based ligands were mainly utilized in asymmetric catalysis. It is documented that functional properties of complexes are largely dependent on the nature of the metal centers and on the bridging ligands and their architectures [2]. Among previously used oxazoline-containing ligands, heteroatom-containing ones, such as pyridyl-oxazolines and phosphoryl-oxazolines, have been proven as reliable candidates for the formation of complexes to be used in catalysis [3]. For example, Sun and his co-workers used 1,3-bis(2-oxazolyl)benzene, 1,4-bis(2-oxazolyl)benzene, 4,4'-di(2-oxazolyl)biphenyl, and 1,3,5-tris(2-oxazolyl)benzene to synthesize a series of silver complexes and examined their optical and catalytic properties [4]. Compared with the above mentioned oxazoline-containing ligands, 2,6-di(2-oxazolyl)pyridine and its analogues have several remarkable features in the assembly of complexes: (1) they can adopt several coordination modes which is favorable to structural diversity; (2) the N atom in the pyridyl ring can act as a Lewis base to subtly influence the catalytic performance.

This work selected 2,6-di(2-oxazolyl)pyridine (L^1), 2-[(*S*)-4-phenyl-2-oxazolyl]quinoline (L^2), and 2-[(*S*)-4-isopropyl-2-oxazolyl]quinoline (L^3) as the organic ligands to react with metal salts. Herein we describe the preparation, characterization and properties of three Ag(I) complexes: $\{[Ag_5(L^1)_5](NO_3)_5\}_n$ (**I**), $[Ag(L^2)(NO_3)]$ (**II**), and $[Ag(L^3)(NO_3)(CH_3CN)]$ (**III**). The fluorescence and non-linear optical properties have been investigated.



EXPERIMENTAL

Materials and methods. All commercially available chemicals were of reagent grade and were used as received without further purification. Referring to the literature [2–4], a slightly revised experimental procedure was used to synthesize oxazoline-containing ligands. Elemental analysis of C, H, and N were taken on a Perkin-Elmer 240C elemental analyzer. Infrared spectra (IR) were recorded on a Bruker Vector22 FT-

¹ The article is published in the original.

Table 1. Crystallographic data and structure refinement details for complexes **I–III**

| Parameter | Value | | |
|---|------------------|------------------|-------------------------|
| | I | II | III |
| Crystal system | Monoclinic | Trigonal | Monoclinic |
| Space group | <i>P</i> 2/c | <i>P</i> 32 | <i>P</i> 2 ₁ |
| <i>a</i> , Å | 14.816(4) | 12.094(3) | 7.3357(17) |
| <i>b</i> , Å | 11.371(3) | 12.094(3) | 27.988(6) |
| <i>c</i> , Å | 19.633(6) | 9.874(3) | 8.9946(15) |
| β, deg | 91.326(2) | 90 | 101.860(10) |
| <i>V</i> , Å ³ | 3306.7(16) | 1250.6(5) | 1807.3(6) |
| <i>Z</i> | 2 | 3 | 4 |
| ρ _{calcd} , mg/m ³ | 1.944 | 1.769 | 1.658 |
| <i>F</i> (000) | 1920 | 666 | 912 |
| θ Range, deg | 1.79–27.90 | 3.37–27.45 | 3.18–27.48 |
| Reflections collected | 19883 | 11853 | 17700 |
| Independent reflections (<i>R</i> _{int}) | 7771 (0.0542) | 3813 (0.0248) | 7857 (0.0275) |
| Reflections with <i>I</i> > 2σ(<i>I</i>) | 4895 | 3639 | 7511 |
| Number of refinement parameters | 468 | 235 | 471 |
| Flack parameter | | −0.041(15) | 0.01(2) |
| Goodness-of-fit on <i>F</i> ² | 0.942 | 1.112 | 1.099 |
| <i>R</i> ₁ (<i>I</i> > 2σ(<i>I</i>))* | 0.0664 | 0.0272 | 0.0360 |
| <i>wR</i> ₂ (<i>I</i> > 2σ(<i>I</i>))** | 0.1181 | 0.0561 | 0.0860 |
| Largest diff. peak and hole, <i>e</i> Å ^{−3} | 0.824 and −0.605 | 0.527 and −0.333 | 1.810 and −0.343 |

* $R_1 = \Sigma |F_o| - |F_c| / \Sigma |F_o|$. ** $wR_2 = [\Sigma w(|F_o|^2 - |F_c|^2)] / [\Sigma w(F_o)^2]^{1/2}$, where $w = 1 / [\sigma^2(F_o^2) + (aP)^2 + bP]$, $P = (F_o^2 + 2F_c^2)/3$.

IR spectrophotometer by using KBr pellets. Thermo-gravimetric (TG) analysis was performed on a simultaneous SDT 2960 thermal analyzer under nitrogen atmosphere with a heating rate of 10°C min^{−1}. The second-order non-linear optical (NLO) intensity was estimated by measuring a powder sample of 80–150 mm diameter in the form of a pellet relative to urea. A pulsed Q-switched Nd:YAG laser at a wavelength of 1064 nm was used to generate a second-harmonic-generation signal (SHG) from powder samples. The backscattered SHG light was collected by a spherical concave mirror and passed through a filter that transmits only 532 nm radiation. The luminescence spectra for the powdered solid samples were measured on an Aminco Bowman Series 2 spectrofluorometer with a xenon arc lamp as the light source. In the measurements of emission and excitation spectra the pass width was 5 nm, and all measurements were carried out under the same experimental conditions.

Synthesis of I. A mixture of L^1 (0.10 mmol, 21.7 mg) and $AgNO_3$ (0.10 mmol, 16.99 mg) in 10 mL acetonitrile was stirred for 10 min and then filtered to

give a clear filtrate. Several days later, colorless block crystals suitable for X-ray diffraction analysis were collected by slow diffusion of diethyl ether into the clear filtrate. The yield was 45% (based on L^1).

For $C_{55}H_{55}N_{20}O_{25}Ag_5$ (*M* = 1935.54)

| | | | |
|-----------------|----------|---------|----------|
| Anal. calcd., % | C, 34.13 | H, 2.86 | N, 14.47 |
| Found, % | C, 34.36 | H, 2.66 | N, 14.69 |

IR data (ν, cm^{−1}): 3070 ν(=C—H), 1659 ν(C=N).

Synthesis of II was carried out by the same procedure as used for the preparation of **I**, except that L^2 ligand (0.10 mmol, 27.4 mg) was used instead of L^1 as the starting material. After several days, colorless block crystals suitable for X-ray diffraction analysis were obtained by slow diffusion of diethyl ether into the clear filtrate. The yield was 40% (based on L^2).

For $C_{18}H_{14}N_3O_4Ag$ (*M* = 444.19)

| | | | |
|-----------------|----------|---------|---------|
| Anal. calcd., % | C, 48.67 | H, 3.18 | N, 9.46 |
| Found, % | C, 48.92 | H, 3.46 | N, 9.70 |

IR data (ν, cm^{−1}): 3098 ν(=C—H), 1649 ν(C=N).

Table 2. Selected bond lengths (Å) and angles (deg) for complexes **I**–**III***

| Bond | <i>d</i> , Å | Bond | <i>d</i> , Å |
|-----------------------------|----------------|--------------------------|----------------|
| I | | | |
| Ag(1)–N(2) | 2.159(3) | Ag(1)–N(3) | 2.162(4) |
| Ag(2)–N(5) | 2.145(4) | Ag(2)–N(6) | 2.151(4) |
| Ag(3)–N(8) | 2.132(4) | Ag(3)–N(8) ^{#1} | 2.132(4) |
| II | | | |
| Ag(1)–O(21) | 2.193(2) | Ag(1)–N(1) | 2.194(2) |
| Ag(1)–N(11) | 2.5060(19) | | |
| III | | | |
| Ag(1)–O(3) | 2.334(3) | Ag(1)–N(1) | 2.344(3) |
| Ag(1)–N(3) | 2.409(4) | Ag(1)–N(11) | 2.340(3) |
| Ag(2)–N(4) | 2.354(4) | Ag(2)–N(21) | 2.353(3) |
| Ag(2)–O(6) | 2.398(3) | Ag(2)–N(2) | 2.347(3) |
| Angle | ω , deg | Angle | ω , deg |
| I | | | |
| N(2)Ag(1)N(3) | 175.78(14) | N(5)Ag(2)N(6) | 174.84(15) |
| N(8)Ag(3)N(8) ^{#1} | 179.2(2) | | |
| II | | | |
| O(21)Ag(1)N(1) | 169.31(9) | O(21)Ag(1)N(11) | 116.69(8) |
| N(1)Ag(1)N(11) | 71.32(8) | | |
| III | | | |
| O(3)Ag(1)N(1) | 119.82(9) | O(3)Ag(1)N(3) | 92.99(12) |
| O(3)Ag(1)N(11) | 143.82(9) | N(1)Ag(1)N(3) | 106.44(12) |
| N(1)Ag(1)N(11) | 72.85(10) | N(3)Ag(1)N(11) | 116.93(11) |
| O(6)Ag(2)N(21) | 139.99(9) | O(6)Ag(2)N(2) | 119.31(9) |
| O(6)Ag(2)N(4) | 94.14(12) | N(4)Ag(2)N(21) | 121.56(11) |
| N(2)Ag(2)N(4) | 103.22(13) | N(2)Ag(2)N(21) | 72.65(10) |

* Symmetry transformations used to generate equivalent atoms: ^{#1} 2 – *x*, *y*, 3/2 – *z* (**I**).

Synthesis of III was carried out by the same procedure as used for the preparation of **I**, except that L³ ligand (0.10 mmol, 24.0 mg) was used instead of L¹ as the starting material. After several days, colorless block crystals suitable for X-ray diffraction analysis were obtained by slow diffusion of diethyl ether into the clear filtrate. The yield was 35% (based on L³).

For C₁₇H₁₉N₄O₄Ag (M = 451.23)

Anal. calcd., % C, 45.25 H, 4.24 N, 12.42
Found, % C, 45.01 H, 4.49 N, 12.70

IR data (ν, cm^{–1}): 3032 ν(=C–H), 1642 ν(C=N).

X-ray structure determinations. The crystallographic data collections were carried out on a Bruker Smart ApexII CCD area-detector diffractometer for **I**

and on a Rigaku Rapid II imaging plate area detector for **II** and **III** using graphite-monochromated MoK_α radiation ($\lambda = 0.71073$ Å) at 200 K. The diffraction data were integrated by using the program SAINT [5], which was also used for the intensity corrections for Lorentz and polarization effects. Semi-empirical absorption corrections were applied using the program SADABS [6]. The structures of **I**–**III** were solved by Direct Methods, and all non-hydrogen atoms were refined anisotropically on *F*² by the full-matrix least-squares techniques using the SHELXL-97 crystallographic software package [7]. All hydrogen atoms at C atoms were generated geometrically. The details of crystal parameters, data collection, and refinements are summarized in Table 1, selected bond lengths and angles are listed in Table 2.

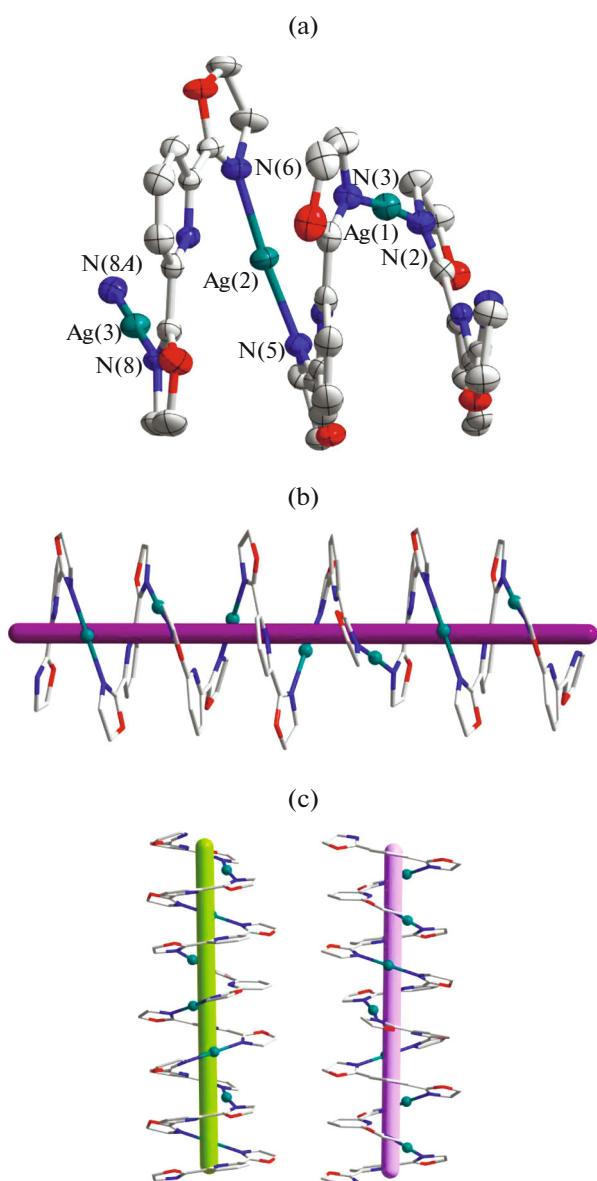


Fig. 1. Coordination environment of Ag(I) in complex **I** with ellipsoids drawn at the 30% probability level (hydrogen atoms and anions of NO_3^- are omitted for clarity, symmetry codes: (A) $2 - x, y, 3/2 - z$ (a); the chain structure of **I** (b); the different helical direction chain in **I** (c).

Supplementary material has been deposited with the Cambridge Crystallographic Data Centre (CCDC nos. 1553091 (**I**), 1553092 (**II**), and 1559788 (**III**); deposit@ccdc.cam.ac.uk or <http://www.ccdc.cam.ac.uk>).

RESULTS AND DISCUSSION

The asymmetric unit of **I** contains 2.5 Ag(I) cations, 2.5 L^1 ligands, and 2.5 NO_3^- anions. Each Ag(I) cation is two-coordinated by two nitrogen atoms from two different L^1 ligands to furnish a nearly linear coordination geometry $[\text{AgN}_2]$ (Fig. 1a). The Ag–N bond lengths are from 2.132(4) to 2.162(4) Å, and the NAGN bond angles are in the range of 174.84(15)° to 179.2(2)° (Table 2). It is noteworthy that the distances of adjacent Ag···Ag pairs range from 3.188 to 3.345 Å, which are shorter than the sum of van der Waals radius (4.06 Å) [8]. The L^1 ligand contains three N atoms, but in **I** the N atom of the pyridine ring is free of coordination, and thus L^1 just acts as a μ_2 -bridge. The C–C single bonds between pyridine and oxazoline can rotate to different angles to satisfy coordinating requirements. In **I**, the two N atoms of the oxazolyl rings protrude from the pyridyl plane towards opposite sides. The interconnection of twisted L^1 units and Ag(I) leads to a helical chain structure (Fig. 1b). However, there exist two different directions of the spiral chain in **I**, left- and right-handed (Fig. 1c). Thus, the crystals of **I** show an achiral meso structure.

In discrete mononuclear units of **II** (Fig. 2a), the silver atom is three-coordinated by two N atoms and one O atom. The L^2 ligand adopts the μ_2 -bidentate chelating coordination mode. The two Ag–N distances are very different (2.194(2) and 2.5059(18) Å). Nitrate acts as counterion and takes part in coordination.

The asymmetric unit of **III** contains two $\text{Ag-L}^3-(\text{NO}_3)$ units (Fig. 2b), within which each Ag(I) is five-coordinated by two N atoms from L^3 , two O atoms from NO_3^- , and one N atom from acetonitrile to furnish a tetragonal pyramidal coordination geometry $[\text{AgN}_3\text{O}_2]$. In **III**, both L^3 and NO_3^- show a μ_2 -bidentate chelating coordination mode, and acetonitrile acts as monodentate ligands.

Complexes **I**–**III** were subjected to thermogravimetric (TG) analyses in N_2 atmosphere to ascertain their thermal stability. The TG curves were recorded from 30 to 600°C (Fig. 3). In the TG curves of **I** and **II**, no obvious weight loss can be observed prior to the decomposition of the crystal framework, which further confirms the absence of solvent in the structures. However, in the TG curve of **III** there is a weight loss of 9.4% within the temperature range of 105 to 130°C corresponding to the release of coordinated acetonitrile (calcd. 9.1%). The decomposition of the frameworks of **I**–**III** occurs at about 268, 227, and 235°C, respectively.

It is known that non-centrosymmetric structures may exhibit second-order NLO effects [9]. The optical properties of **II** and **III** were investigated to evaluate their potential application as second-order NLO

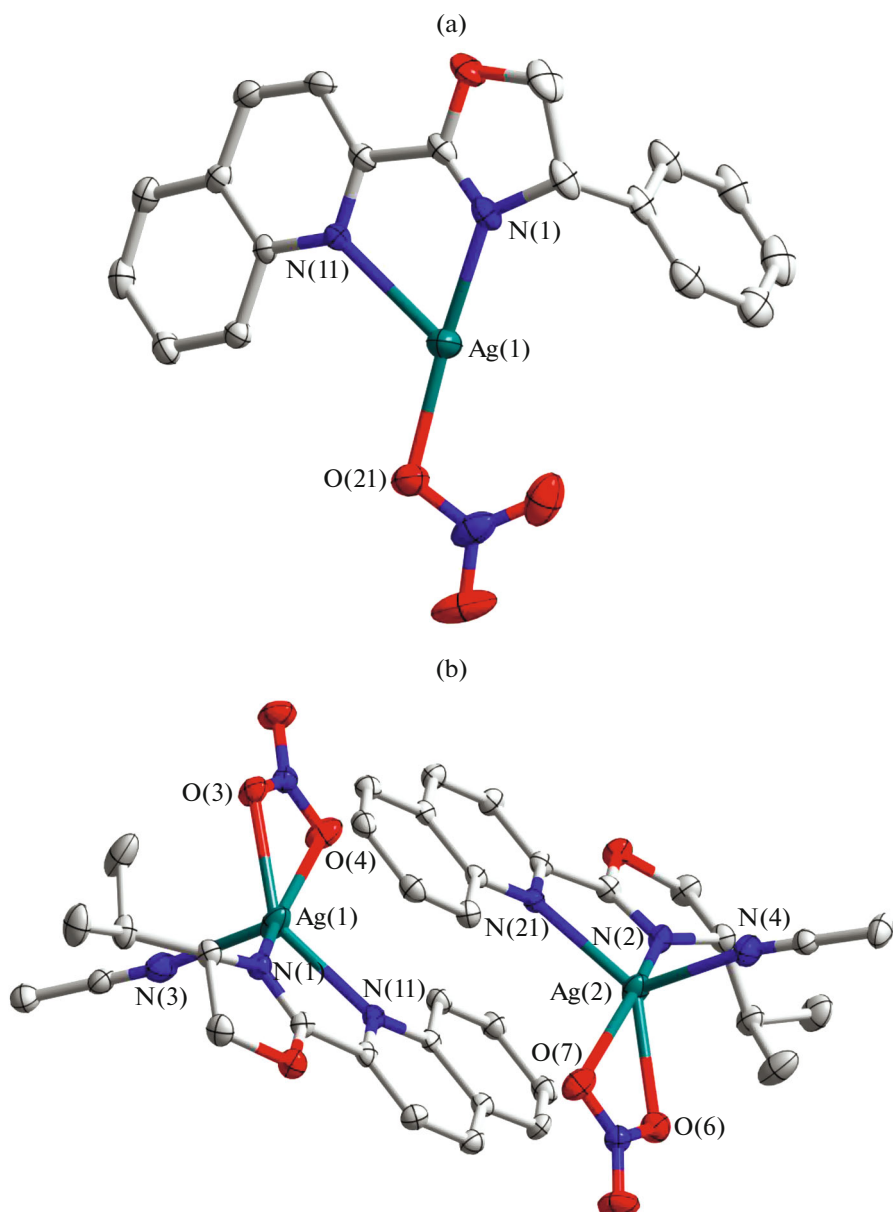


Fig. 2. Molecular structure of **II** (a) and **III** (b) and coordination environment of Ag(I) in **II** (a) and **III** (b) with ellipsoids drawn at the 30% probability level; hydrogen atoms are omitted for clarity.

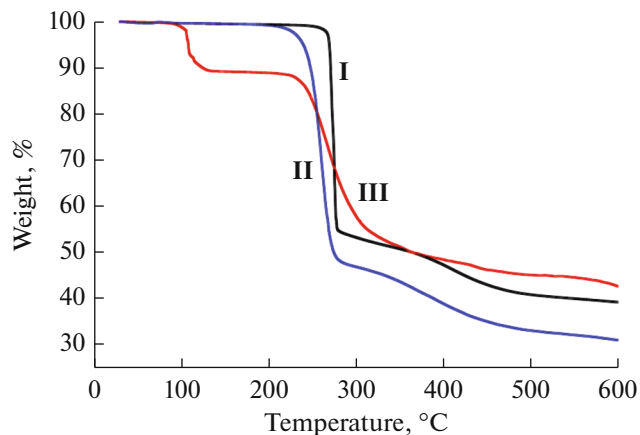


Fig. 3. TG curves of complexes **I–III**.

materials. Approximate estimations were carried out using a pulsed Q-switched Nd:YAG laser at a wavelength of 1064 nm. The result obtained from powdered samples (80–150 μ m diameters) in the form of a pellet (Kurtz powder test) was compared with that obtained for urea. Complexes **II** and **III** exhibit powder SHG intensities comparable to that for urea with the response of 0.6 and 0.9 times, respectively.

Previous studies have shown that inorganic-organic hybrid coordination polymers containing metal centers with d^{10} electron configuration such as Ag(I) exhibit excellent luminescent properties and may have potential applications as photoactive materials [10, 11]. In the present work, the photolumines-

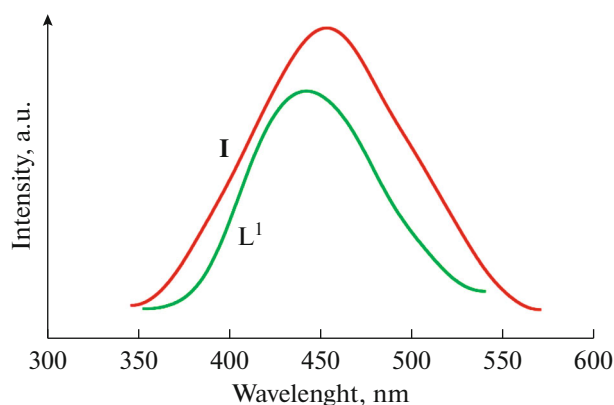


Fig. 4. Emission spectra of **I** and the L^1 in the solid state at room temperature.

cence of complex **I** and ligand L^1 has been recorded in the solid state at room temperature. As shown in Fig. 4, intensive emission can be observed under the experimental conditions for the complex and the L^1 ligand with bands at 453 nm ($\lambda_{\text{ex}} = 376$ nm) and at 442 nm ($\lambda_{\text{ex}} = 360$ nm), respectively. The fluorescent emission of the complex may be tentatively assigned to intra-ligand transitions of coordinated ligands, since similar emission was observed for the free ligand [12, 13]. The observation of a red shift of the emission maximum in complex **I** compared with the free ligand may originate from the coordination of the ligands to the metal centers [14, 15].

ACKNOWLEDGMENTS

The authors gratefully acknowledge Natural Science Foundation for Universities in Jiangsu Province (16KJB150005) and Huaiyin Institute of Technology

(15HGZ006 and 491713325) for financial support of this work.

REFERENCES

1. Kuai, H.W., Lv, G.C., Hou, C., et al., *J. Solid State Chem.*, 2015, vol. 223, p. 2.
2. Kuai, H.W., Xia, J.J., and Sang, H.Y., *Inorg. Chem. Commun.*, 2016, vol. 72, p. 73.
3. Kuai, H.W., Cheng, X.C., Li, D.H., et al., *J. Solid State Chem.*, 2015, vol. 228, p. 65.
4. Zhao, Y., Chen, Y., Fan, J., et al., *Dalton Trans.*, 2014, vol. 43, no. 5, p. 2252.
5. *SAINT, Program for Data Extraction and Reduction*, Madison: Bruker AXS, Inc., 2001.
6. Sheldrick, G.M., *SADABS, Program for Bruker Area Detector Absorption Correction*, Göttingen: Univ. of Göttingen, 1997.
7. Sheldrick, G.M., *SHELXS/L-97, Programs for the Determination of Crystal Structure*, Göttingen: Univ. of Göttingen, 1997.
8. Hu, S.Z., Zhou, Z.H., and Tsai, K.R., *Acta Phys. Chim. Sin.*, 2003, vol. 19, no. 11, p. 1073.
9. Hou, C., Liu, Q., and Lu, Y., *Microporous Mesoporous Mater.*, 2012, vol. 152, p. 96.
10. Kuai, H.W., Xia, J.J., Li, D.H., et al., *Russ. J. Coord. Chem.*, 2017, vol. 43, no. 7, p. 473. doi 10.1134/S1070328417070065
11. Dai, C.H. and Mao, F.L., *Russ. J. Coord. Chem.*, 2015, vol. 41, no. 6, p. 405. doi 10.1134/S1070328415060020
12. Huang, Y.Q., Ding, B., Song, H.B., et al., *Chem. Commun.*, 2006, vol. 10, no. 47, p. 4906.
13. Valeur, B., *Molecular Fluorescence: Principles and Applications*, Weinheim (Germany): Wiley-VCH, 2002.
14. Zhang, L., Li, Z.J., and Lin, Q.P., *Inorg. Chem.*, 2009, vol. 48, no. 14, p. 6517.
15. Wang, X.L., Bi, Y.F., Liu, G.C., et al., *CrysEngComm*, 2008, vol. 9, no. 10, p. 349.